

FIGURE 2: Reaction scheme for zinc-activated hydroxide displacement of -NH_2 from C-4 of the pyrimidine ring, showing the role of the carboxyl group of Glu-104 at several stages of the reaction.

consistent with the idea that polar interactions are involved in substrate activation. Information about the state of bond making and breaking in the transition state has been lacking.

Recently, viscosity variation experiments showed that the barriers for substrate binding and product release have no kinetic significance for the action of this enzyme, indicating that K_m represents a true dissociation constant of the ES complex and that k_{cat} describes the chemical conversion of the ES complex to the EP complex (10). These results suggest that kinetic isotope studies could afford a transition state analysis of the mechanism of cytidine deaminase.

In the present work, we measured the primary ^{15}N isotope effects by following the changes in the natural abundance of ^{15}N in the ammonia formed, for both the uncatalyzed and enzyme-catalyzed deaminations of cytidine. The results of these experiments were used to determine whether the two reactions proceed by the same mechanism in solution, and to compare the results with mechanisms previously proposed for adenosine (12) and AMP (13) deaminases. Effects of D_2O , pH, and enzyme variants Glu91Ala, His102Ala, and His102Asn on $^{15}(\text{V}/\text{K})$ were also measured to allow more detailed characterization of the postulated tetrahedral intermediate generated by zinc-activated hydroxide attack at C-4 of the pyrimidine ring. In addition, ^{15}N isotope effects were measured for pyrimidine N-3, again by internal competition.

EXPERIMENTAL PROCEDURES

Materials. Wild-type and site-directed mutant cytidine deaminases were purified from cell extracts of *Escherichia coli* SS6130 as described previously (14). This strain is unable to express the endogenous *cdd* gene and completely derepresses the expression of the plasmid-borne *cdd* gene,

allowing cytidine deaminase to be expressed from only the plasmid-borne gene. Concentrations of enzyme stocks (found to be greater than 95% homogeneous as analyzed by SDS-PAGE) were determined from the absorbance at 280 nm using an extinction coefficient of $3.9 \times 10^4 \text{ M}^{-1} \text{ cm}^{-1}$ (15). Cytidine and 3'-deoxycytidine were purchased from Sigma. 1-Methylcytosine was synthesized and characterized by UV and NMR by the method of Helfer et al. (16).

Isotope Effect Nomenclature. The nomenclature used in this work is that of Northrop (17) in which $^{15}(\text{V}/\text{K})$ represents the ratio of the V/K for ^{14}N -containing species to that of ^{15}N -containing species.

Primary $^{15}(\text{V}/\text{K})$ for Enzymatic Deamination of Cytidine. The primary ^{15}N kinetic isotope effect for cytidine deamination was determined by isotope ratio mass spectrometric analysis of the ammonia (subsequently converted to N_2) produced from complete or partial conversions of cytidine to ammonia by the use of natural abundance ^{15}N at the exocyclic leaving group nitrogen. The observed ^{15}N kinetic isotope effect at the pyrimidine N-3 in uridine was determined by degradation of uridine and isolation of N-3 as ammonia (subsequently converted to N_2). The complete conversion of cytidine to uridine and ammonia provides the $^{15}\text{N}/^{14}\text{N}$ ratio of the substrate. Partial conversions (15–50%) of cytidine to uridine and ammonia reflect the isotopic discrimination. Typically, solutions of 20–50 mL of potassium phosphate buffer (0.10 M, pH 7.3) and cytidine, or 3'-deoxycytidine (0.020 M) were adjusted to pH 11–12 with KOH and degassed to remove exogenous ammonia, and then readjusted to pH 7.3 with 18 M H_2SO_4 . Cytidine deaminase (wild-type or mutant enzyme) was then added, and the extent of reaction was monitored spectrophotometrically by comparing the decrease in absorbance at 282 nm with that at the isosbestic point at 268 nm. Nessler's reagent was used to confirm that the concentrations of ammonia produced matched the extent of reaction determined spectrophotometrically. After 15–50% conversion of cytidine to uridine, the reactions were quenched by adjustment with 18 M H_2SO_4 to pH ~ 1.5 . In the 100% conversion samples, the reaction was continued until conversion of cytidine to uridine was complete, followed by the adjustment with 18 M H_2SO_4 to pH ~ 1.5 .

To determine the $^{15}\text{N}/^{14}\text{N}$ ratio at N-3 of the pyrimidine ring in the product, uridine was separated from cytidine by anion-exchange chromatography by the method of Cohn (18). Reaction samples were diluted with column equilibration buffer (0.2 M NH_4OH + 0.025 M NH_4Cl , pH 10.6) and loaded onto a DOWEX trimethylbenzylammonium anion exchange column (4 \times 30 cm) in the hydroxide form. Cytidine was completely eluted from the column in the flow-thru, and uridine was batch-eluted using 1 mM HCl. This method afforded >90% recovery of the uridine (> 100 mmol) produced by enzymatic deamination as determined spectrophotometrically. Solutions containing uridine were combined and titrated to pH 7 with KOH, evaporated to dryness under reduced pressure, redissolved in water, filtered (0.2 μm), desalted on a Alltech Econosil HPLC C18 column (2.2 \times 25 cm), and eluted in 5% methanol. Ammonia was then specifically liberated from the pyrimidine N-3 by hydrolysis with 6 N HCl (19).

Ammonia was isolated from the samples using steam distillation (20) with the following exceptions. The sample

was first added to the inlet reservoir flask with enough volume (45 mL) to cover the steam inlet, and then the sample's pH value was adjusted to 10.5 with 10–20 mL of 3 M Na₂CO₃, using a syringe through a septum. Using stronger alkali (13 N KOH) promoted further deamination or pyrimidine degradation, and therefore was not used. The volume was reduced under vacuum (20 mmHg) at 40 °C. The ammonia was oxidized to N₂(g) with NaOBr (aq), isolated and then analyzed using a Finnegan Mat Delta isotope ratio mass spectrometer as described by Rishavy et al. (21).

Solvent D₂O Effects on k_{cat} and k_{cat}/K_m . Initial velocity studies were performed in quadruplicate at 25 °C in potassium phosphate buffers (0.1 M, pH(D) 7.3) using a continuous spectrophotometric assay for measuring the rate of cytidine conversion to uridine ($[S] > 10 \times K_m$, $\Delta\epsilon_{298\text{ nm}} = -120\text{ M}^{-1}\text{ cm}^{-1}$; $[S] < 0.1 \times K_m$, $\Delta\epsilon_{282\text{ nm}} = -3600\text{ M}^{-1}\text{ cm}^{-1}$). The mole fraction deuterium ranged from 0 to ~0.98 using potassium phosphate exchanged 3× in D₂O and stocks of cytidine prepared in D₂O. Values of pD were obtained by adding 0.40 to the observed reading of the pH meter (22).

Primary ¹⁵N Kinetic Isotope Effects for Uncatalyzed 1-Methylcytosine Deamination. Solutions of 1-methylcytosine (0.024 M) were degassed at pH ~11 to remove exogenous ammonia, and then placed in potassium phosphate buffer (0.25 M, pH 7.3) and heated (100–190 °C) in PTFE-lined acid digestion bombs. The more basic reaction mixtures (pH 12.5, 0.25 M potassium phosphate) were heated at 100 °C. After varying time periods (0.5–340 h), the bombs were chilled on ice, and 18 M H₂SO₄ was added to the solutions (to pH~2) to trap the generated ammonia. The extent of deamination was determined spectrophotometrically and was found to proceed to completion following simple first-order kinetics with a rate constant that closely approximated the value established for cytidine deamination (10). The ¹⁵N/¹⁴N ratio of product ammonia was determined as described above.

To examine the effect of water concentration on the spontaneous rate of deamination, aqueous solutions of 1-methylcytosine and potassium phosphate buffer (pH 7.3) were mixed with DMSO or DMF so that the final concentrations of buffer (50 mM) and 1-methylcytosine (10 mM) remained constant for each sample. The samples were then sealed in quartz tubes (2 mm internal diameter, 1 mm wall thickness) and heated at 145 °C for varying time periods (12–24 h). After the reactions were chilled on ice, the extent of reaction was determined by diluting a small reaction aliquot (10 µL) into 3 mL of potassium phosphate buffer (0.1 M, pH 7.3) to measure the change in UV absorbance as described above. Reported rate constants are the average of three independent reactions.

Data Analysis. The ¹⁵N kinetic isotope effect was determined using eq 1,

$$\text{KIE} = \log(1 - f)/\log(1 - fR_p/R_o) \quad (1)$$

where f is the fraction of reaction, R_p is the ¹⁵N/¹⁴N ratio in the product, and R_o is the mass ratio in the initial substrate (determined by 100% conversion to product ammonia).

RESULTS AND DISCUSSION

¹⁵N Isotope Effects for Cytidine Deaminase. The catalytic mechanism of cytidine deaminase is proposed to involve a

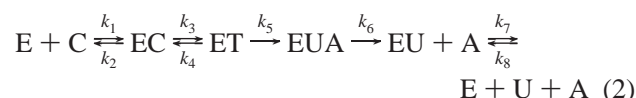
Table 1: Primary ¹⁵N Kinetic Isotope Effects for Cytidine Deaminase^a

enzyme ^b	substrate	solvent	pH(D)	k_{cat}/K_m (M ⁻¹ s ⁻¹)	¹⁵ (V/K) ± SE	<i>n</i> ^c
Exocyclic NH ₂						
wt	cytidine	H ₂ O	7.3	3.0×10^6	1.0109 ± 0.0001	10
wt	cytidine	D ₂ O	7.3	4.7×10^6	1.0086 ± 0.0002	6
wt	cytidine	H ₂ O	4.2	1.7×10^5	1.0123 ± 0.0001	6
wt	3'-deoxy- cytidine	H ₂ O	7.3	4.0×10^2	1.0083 ± 0.0003	4
E91A	cytidine	H ₂ O	7.3	1.5×10^2	1.0124 ± 0.0001	7
H102A	cytidine	H ₂ O	7.3	3.8×10^2	1.0134 ± 0.0003	7
H102N	cytidine	H ₂ O	7.3	5.3×10^4	1.0158 ± 0.0002	8
Pyrimidine N-3						
wt	cytidine	H ₂ O	7.3	3.0×10^6	0.9879 ± 0.0006	5

^a In 50 mM potassium phosphate buffer (pH 7.3) or 50 mM sodium acetate buffer (pH 4.2) at 25 °C. ^b Wild-type (wt) or mutant cytidine deaminases. ^c Number of determinations.

tetrahedral intermediate, formed by zinc-bound hydroxide attack at C-4 of the pyrimidine ring (Figure 2). This mechanism is supported by this enzyme's potent inhibition by substrate analogues that contain a tetrahedral carbon atom at the position of substitution and by the enzyme's ability to catalyze formation of tightly bound analogues of this type (23).

The simplest enzymatic mechanism can be written as follows:



where E is the enzyme, C is substrate cytidine, EC is the Michaelis complex, T is the tetrahedral intermediate formed by the addition of hydroxide to C, and U and A represent products uridine and ammonia, respectively. Inhibition by ammonia of adenosine deaminase ($K_i \sim 0.04\text{ M}$) was found to be noncompetitive, suggesting that NH₃ release occurs prior to the release of inosine during catalysis (24). Cytidine deaminase shows a much weaker affinity for ammonia ($K_i > 1\text{ M}$) (25), suggesting that ammonia's rate of dissociation is rapid and virtually irreversible. Moreover, the action of cytidine deaminase is not limited by substrate binding or product release, as shown by viscosity variation studies with trehalose (10). Therefore, the primary ¹⁵N isotope effects measured for CDA are affected only by steps leading up to the irreversible release of ammonia and should be sensitive to the formation (k_3) and breakdown (k_4 and k_5) of the tetrahedral intermediate.

The ¹⁵N isotope effect for the exocyclic amino group, released as ammonia in the conversion of substrate to product, with wild-type CDA, is 1.0109 ± 0.0001 (Table 1). The size of this isotope effect suggests that C–N cleavage at least partially limits the rate of enzymatic deamination. As shown below, the suppression of the isotope effect by a forward commitment can be removed or reduced by varying pH or by using enzyme variants with reduced catalytic activity.

Adenosine deaminase, ADA, is similar to CDA in active site structure and in the rate enhancement it produces (1, 26). The ¹⁵(V/K) in the exocyclic amino group in the adenosine deaminase catalyzed reaction is 1.0041 (12), a factor of ~2.7 smaller than the effect observed for CDA. The action of ADA on the slow substrate, 7,8-dihydro-8-

oxoadenosine, showed a larger ^{15}N isotope effect of 1.0150, and is presumably limited by a chemical, rather than physical or binding, process. The $^{15}(\text{V}/K)$ for AMP deaminase, which is subject to allosteric activation by ATP, ranged from 1.010 (without ATP) to 1.016 (with ATP) and was 1.013 for its action on ATP, a slow substrate (13).

Cytidine deaminase's catalytic efficiency ($k_{\text{cat}}/K_{\text{m}}$) was previously found to decrease with increasing acidity below pH 6 (9), giving an 18-fold smaller value of $1.7 \times 10^5 \text{ M}^{-1} \text{ s}^{-1}$ at pH 4.2 than pH 6, suggesting that chemistry becomes more rate determining at lower pH values where incorrect protonation of the catalytic groups slows the chemical step. In accord with that view, the $^{15}(\text{V}/K)$ isotope effect increased from 1.0109 (pH 7.3) to 1.0123 ± 0.0001 at pH 4.2, showing that the intrinsic isotope effect due to C–N bond cleavage was partially masked in neutral solution and that commitments due to pH effects on proton transfers were reduced at pH 4.2.

Several mutant cytidine deaminases have also been characterized kinetically to determine the effect of mutation on catalytic efficiency and transition state stabilization. The crystal structure of the enzyme complex with 5-fluoro-3,4-dihydrouridine (a transition state analogue) shows that zinc is coordinated by one histidine (H102) and two cysteine (C129 and C132) residues (Figure 1) (4). The activated substrate water, in the form of hydroxide, coordinates the fourth ligand site of zinc. Site-directed mutagenesis of these residues produced enzyme variants with reduced zinc affinity and reduced catalytic activity (7). Of these enzyme mutants, His102Ala and His102Asn were stable proteins that regained partial activity when preincubated with zinc and showed maximal activity at 1 mol of zinc:1 mol of enzyme subunits. Their reduced catalytic efficiency was largely due to reductions in k_{cat} , with little effect on K_{m} . The value of $^{15}(\text{V}/K)$ was found to increase for the His102Ala mutant from 1.0109 (wild-type) to 1.0134 ± 0.0003 , and to 1.0158 ± 0.0002 for the His102Asn mutant. This relatively larger ^{15}N kinetic isotope effect for the His102Asn mutant indicates that the commitments have likely been eliminated. Since the $-\text{NH}_2$ of the tetrahedral intermediate can only be eliminated after protonation by Glu-104, this elimination should have an early transition state. Even so, the isotope effect observed is large and presumably reflects the intrinsic isotope effect on C–N cleavage, multiplied by an equilibrium isotope effect for forming the protonated $-\text{NH}_3^+$ group from the $-\text{NH}_2$ group of cytidine. Because this equilibrium isotope effect is known and inverse (0.9836) (20), we can calculate an intrinsic isotope effect of 1.033 for C–N bond cleavage.

"Snapshots" taken of the enzyme's action along the reaction coordinate, from structural data of enzyme complexes with a substrate analogue (3), transition state analogues (4, 5), and product uridine (6) show that the ribose is held in a fixed position while the pyrimidine ring moves toward the zinc-bound hydroxide and away from ammonia. Thus, the ribofuranosyl group acts as an anchor during the catalytic process.² Disruption of an H-bond that mediates contact between the anchor and the enzyme, by removing the OH group on the substrate, producing 3'-deoxycytidine, or by mutating the enzyme (Glu91Ala), causes a reduction

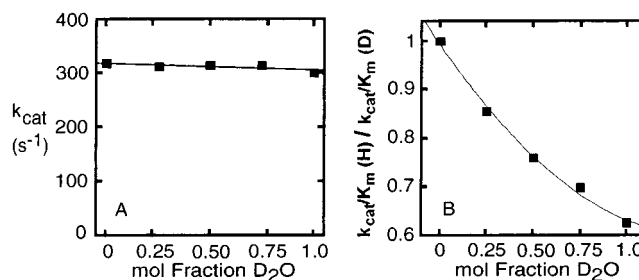


FIGURE 3: Effects of solvent D_2O on (A) k_{cat} and (B) $k_{\text{cat}}/K_{\text{m}}$ for wild-type cytidine deaminase acting on cytidine, in potassium phosphate buffer [0.1 M, pH(D) 7.3] at 25 °C.

in catalytic efficiency by a factor of $\sim 10^4$ (8). This results in a positive change in the entropy of transition state binding, suggesting that the anchor has lost its grip (10). For the action of mutant enzyme Glu91Ala on cytidine, the value of $^{15}(\text{V}/K)$ increases from 1.0109 to 1.0124 ± 0.0001 , as expected for a less efficient chemical process in which the ET complex partitions back to the EC complex more frequently than it partitions forward to the EUA complex. However, the ^{15}N kinetic isotope for the slow substrate 3'-deoxycytidine actually decreases to 1.0083 ± 0.0003 . Although the rate of binding of 3'-deoxycytidine by CDA is relatively rapid as compared to an internal step,³ the lowered $^{15}(\text{V}/K)$ suggests that changes in a partition ratio of a prior step to ammonia elimination increases the commitment to C–N bond breakage. The much lower k_{cat} may be the result of unproductive binding, which lowers the observed value of k_{cat} but does not affect the value of $^{15}(\text{V}/K)$. Thus, even though disrupting this interaction remote to chemical transformation by either method produces almost equivalent decreases in transition state stabilization, the intrinsic partitioning of the intermediates is different in the two cases.

Solvent Deuterium Isotope Effects. Increasing the deuterium content of the solvent is found to have little effect on k_{cat} for the wild-type enzyme (Figure 3A). In contrast, the effect of solvent D_2O on $k_{\text{cat}}/K_{\text{m}}$ was found to be inverse (Figure 3B). A proton inventory (fractional change in rate with fractional change of D_2O content) for $k_{\text{cat}}/K_{\text{m}}$ is curved showing that two or more protons increase their fractionation factors in going to the transition state. These are presumably the protons on Zn-bound water, which become bonded to N-3 and to the exocyclic amino group in the ET complex. These data suggest that the proton from $\text{Zn}-\text{OH}_2$ does not shift to Glu-104 until cytidine binds.

In D_2O , the primary $^{15}(\text{V}/K)$ decreases to 1.0086 ± 0.0002 from 1.0109 in H_2O . The fact that the ^{15}N kinetic isotope effect decreases in D_2O rules out mechanisms in which there is only one kinetically significant step (28). Deuterium oxide had the same effect on $^{15}(\text{V}/K)$ for adenosine and AMP deaminases, so that these reactions also do not occur in a concerted fashion, in accord with the proposed mechanism involving an addition–elimination sequence.

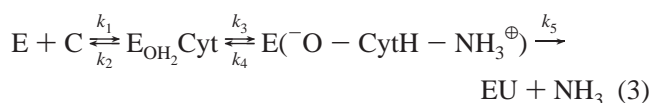
Pyrimidine N-3 ^{15}N Isotope Effects. It is proposed that the nitrogen atom at position 3 in the pyrimidine ring accepts a proton from Glu-104 and undergoes rehybridization from sp^2

² For a discussion of the anchor principle, see ref 27.

³ Earlier viscosity variation experiments showed no substantial effect on $k_{\text{cat}}/K_{\text{m}}$ of wt CDA with 3'-deoxycytidine, suggesting that its reduced catalytic efficiency was due to a chemical step becoming more rate limiting (10).

to sp³ during transformation to uridine (Figure 2). The ¹⁵(V/K) value at N-3 showed an inverse effect of 0.9879 ± 0.0006 or 1.2% as expected for protonation of N-3 in a step prior to ammonia elimination.⁴ It is likely that N-3, with a pK_a value of 4.6 in the ground state, is protonated and rehybridized as the Zn-coordinated hydroxide attacks C-4 to form the tetrahedral intermediate, although it is possible that protonation of N-3 precedes hydroxide attack. The observed inverse effect must be the product of an equilibrium and a kinetic effect. The equilibrium isotope effect for protonation of N-3 is inverse, although if protonation is concerted with attack of hydroxide, the observed isotope effect will be less inverse than the full equilibrium isotope effect. In that process, the pK_a value of N-3 will be raised by the increase of electron density through the ring as the hydroxide approaches C-4 (29) and by deformation of the pyrimidine ring as C-4 changes from sp² to sp³ hybridization.

Intrinsic Isotope Effect Analysis. For the His102Asn mutant, it seems reasonable to infer that the rate-limiting step of enzymatic deamination is the breakdown of the tetrahedral intermediate to products (NH₃ elimination). The transition state for ammonia elimination should be fairly early, so the isotope effect of 1.6% measured for the H104N is consistent with no commitments. On the basis of the equations derived by Weiss (12), an intrinsic isotope analysis for the enzymatic mechanism can be accomplished using a simplified form of eq 2:



Assuming D and ¹⁵N isotope effects on k₃, k₄, and k₅, but accounting for the lack of stickiness of the substrate (10), the following equations apply to the mechanism in eq 3.

$$^{15}(V/K)_H = \frac{^{15}K_{eq3} \ ^{15}k_5 + ^{15}k_3 \left(\frac{k_5}{k_4}\right)}{1 + \left(\frac{k_5}{k_4}\right)} \quad (4)$$

$$^{15}(V/K)_D = \frac{^{15}K_{eq3} \ ^{15}k_5 + ^{15}k_3 \left(\frac{k_5}{k_4}\right) \left(\frac{^Dk_4}{^Dk_5}\right)}{1 + \left(\frac{k_5}{k_4}\right) \left(\frac{^Dk_4}{^Dk_5}\right)} \quad (5)$$

The solvent deuterium isotope effect will be

⁴ To pursue the possibility that a LBHB exists between the 4-OH group of the tetrahedral intermediate and Glu 104, ¹H NMR spectra of CDA (1.6 mM) and a transition state analogue, 3,4-dihydrouridine, in phosphate buffer (50 mM, pH 7.0) was acquired. The X-ray structure (5) of this complex showed a possible short hydrogen bond distance between the hydroxide proton at C-4 of 3,4-dihydrouridine and the Glu 104 carboxylate ion. However, the ¹H NMR spectra (750 MHz) did not reveal any new peaks accompanying ligand binding in the downfield region with 3,4-dihydrouridine at concentrations of 1.4 and 2.8 mM.

$$^D(V/K) = \frac{^DK_{eq5} \ ^Dk_5 + ^Dk_3 \left(\frac{k_5}{k_4}\right)}{1 + \left(\frac{k_5}{k_4}\right)} \quad (6)$$

The ¹⁵N sensitive steps for the exocyclic amino group are formation of the tetrahedral intermediate and its breakdown. The protonation of -NH₂ to become -NH₃⁺ occurs before ammonia is eliminated, and transfer is included in the ¹⁵K_{eq3} term which was determined as 0.9836 (20). The kinetic isotope effect for the step that includes protonation of the amino group (k₃) is likely to be close to unity, even though ¹⁵K_{eq3} is inverse, since it involves N-H bond formation and is thus a primary isotope effect. Using 1.0158 from the H102N mutant as ¹⁵K_{eq3}¹⁵k₅ and assuming no external commitments⁵ at pH 4.2, eq 4 with the data for wild-type cytidine deaminase at this pH becomes:

$$1.0123 = \frac{1.0158 + \left(\frac{k_5}{k_4}\right)}{1 + \left(\frac{k_5}{k_4}\right)} \quad (7)$$

Solving for k₅/k₄ gives 0.29 at pH 4.2. At neutral pH, there is a change in the internal commitment from that at pH 4.2, since the observed isotope has decreased, and k₃/k₂ is assumed to be small as illustrated by viscosity studies (10). The internal commitment, k₅/k₄, at pH 7.2 can be calculated as 0.45 with eq 7 where 1.0109 replaces 1.0123. The tetrahedral intermediate thus breaks down 2.2 times more often than it is converted to products. The step of C-N bond cleavage is the highest barrier on the reaction coordinate.

The decreased commitment at pH 4.2 is either caused by a decrease in k₅ or an increase in k₄ relative to the values at neutral pH. A decrease in k₅ could represent partial protonation of Glu-104, which is needed to transfer a proton between the -OH and -NH₂ groups of the tetrahedral intermediate. An increase in k₄ might be caused by the same effect.

The deuterium sensitive steps occur before the tetrahedral intermediate breaks down to eliminate ammonia. Using wild-type data at neutral pH, assuming ^Dk₅ = 1 and again that k₃/k₂ is small, eq 5 is:

$$1.0086 = \frac{1.0158 + (0.45)(^Dk_4)}{1 + (0.45)(^Dk_4)} \quad (8)$$

Solving eq 8, ^Dk₄ = 1.86.

The solvent deuterium isotope equation can be solved for ^Dk₃:

⁵ The mutant H102N has a more pronounced ¹⁵N isotope effect at pH 7.3 than the wild type has at pH 4.2. As a higher isotope effect generally indicates lower commitments, the isotope effect for H102N has less commitments than the wild type. Furthermore, its magnitude suggests there is little or no commitment for this mutant. Therefore, it is assumed that the value of ¹⁵k₅¹⁵K_{eq3} is the intrinsic isotope for the wild type.

$$0.63 = \frac{{}^D K_{eq3} + {}^D k_3(0.45)}{1 + 0.45} \quad (9)$$

Thus ${}^D k_3 = 0.92$ and ${}^D K_{eq3} = 0.49$. ${}^D k_3$ is inverse, and therefore an equilibrium isotope effect. This value and the curved proton inventory show that protons are transferred during the k_3 step. These protons are likely to be the one transferred to N-3, which is protonated before ammonia release as shown by its ${}^{15}(V/K)$, and the one transferred to the exocyclic amine in the tetrahedral intermediate. The fractionation factor of the protons on the exocyclic amine in the transition state may be determined by assigning fractionation factors to these protons in the compounds from which they originated, and in the compound they finally resided on, along with the calculated ${}^D K_{eq3}$ value. The unprotonated exocyclic amine should have a fractionation factor of 1.0, while the protons of protonated NH_3 are 1.1. If the protons that originated on the $Zn-OH_2$ have fractionation factors of 0.77 and the proton on N-3 has one of 1.1, the value of ${}^D K_{eq3}$ is matched.

Although the solvent deuterium isotope effect on k_{cat}/K_m is inverse, the solvent deuterium isotope effect on k_{cat} is small. The following analysis of V elucidates the conditions necessary to explain the small isotope effect on k_{cat} when it is known that the chemical steps are rate-limiting (10). Equations 10 and 11 apply to the mechanism in eq 3, when the direct comparison method for measuring isotope effects is used.

$$\frac{V}{E_t} = \frac{k_3 k_5}{k_3 + k_4 + k_5} \quad (10)$$

$${}^D V = \frac{k_3 {}^D k_5 + {}^D K_{eq3} k_4 {}^D k_5 + {}^D k_3 k_5}{k_3 + k_4 + k_5} \quad (11)$$

Solving eq 11 using values of ${}^D k_3$, ${}^D k_4$, ${}^D k_5$, and k_5/k_4 calculated above results in eq 12.

$${}^D V = \frac{k_3 + 2k_5}{k_3 + 3.22k_5} \quad (12)$$

A value for ${}^D V$ of 0.96 is achieved when $k_3 \geq 25k_5$. Rapid formation of the tetrahedral intermediate (k_3), followed by slower C–N bond cleavage (k_5) to products, is consistent with C–N bond cleavage being the major rate-determining step.

Structural Context of Enzymatic Deamination. During the overall conversion of cytidine to uridine, the pyrimidine ring moves away from the leaving group (ammonia) and toward the attacking group (zinc-coordinated hydroxide), describing an arc with respect to the ribofuranosyl group that remains anchored in position (6). Glu-104 appears to be the key residue that facilitates the flow of electrons for cytidine deamination within the confines of the enzyme's active site. In the enzyme's complex with the transition state analogue 3,4-dihydrouridine, Glu-104 forms two hydrogen bonds with this analogue's 4-OH and 3-NH groups (Figure 1). These bonds require that the carboxyl group of Glu-104 lie in the plane of the pyrimidine ring at this stage of the reaction. The present results show that water addition is not rate-determining. As the corresponding tetrahedral intermediate

Table 2: Primary ${}^{15}N$ Kinetic Isotope Effects for Spontaneous Deamination of 1-Methylcytosine^a

temp (°C)	pH	k_{non} (s ⁻¹)	KIE \pm SE	n^b
100–185	7.0	varies ^c	1.0021 ± 0.0002	26
100	12.5	1.1×10^{-5}	1.0035 ± 0.0002	5

^a In 0.1 M potassium phosphate buffers. ^b Number of determinations. ^c First-order rate constants increase from $6.3 \times 10^{-7} \text{ s}^{-1}$ (100 °C) to $1.5 \times 10^{-4} \text{ s}^{-1}$ (185 °C).

partitions forward to products uridine and ammonia in the rate-determining step, Glu-104 is in a good position to transfer the proton from the added OH group to incipient ammonia (Figure 2). As this transfer occurs, the carboxylate group of Glu-104 appears to rotate in such a way as to retain contact with the 3-NH group of the developing uridine. One oxygen atom of Glu-104 assists the release of ammonia, as the other oxygen atom (through its interaction with the 3-NH group) draws the pyrimidine ring toward zinc, generating the enzyme–uridine complex.

Uncatalyzed Deamination of 1-Methylcytosine. Enzymatic deamination of cytidine occurs $\sim 10^{12}$ times more rapidly than the uncatalyzed reaction (1, 10). This rate enhancement (k_{cat}/k_{non}) also reflects the enzyme's differential binding affinity for the substrate in its activated form in the transition state relative to the ground state (K_{tx}/K_m) (2). Transition state affinity is underestimated if the uncatalyzed and enzyme-catalyzed reactions proceed by different mechanisms.⁶ To determine whether CDA uses a different mechanism to catalyze the hydrolytic deamination of cytidine, we measured the primary ${}^{15}N$ isotope effect on the nonenzymatic hydrolysis of 1-methylcytosine. This analogue of cytidine was used to avoid cleavage of ribose from N-1 that would occur under these conditions. 1-Methylcytosine was observed to undergo hydrolytic deamination at elevated temperatures in neutral solution by a simple first-order process at rates that matched those previously determined for cytidine (10). At temperatures between 100 and 185 °C, the ${}^{15}N$ isotope effect was 1.0021 ± 0.0002 at pH 7.0 (Table 2). This much smaller isotope effect, relative to that of the enzyme-catalyzed reaction (1.0109), shows that the uncatalyzed reaction has higher forward commitments. This may be attributed to the required proton transfer from the attacking water via a H-bonding network to N-3 in the pyrimidine ring that must occur during addition at C-4. Once the tetrahedral intermediate is formed, it reacts to eliminate NH_3 faster than it expels water, i.e., the proton shift from N-3 to the OH may be hindered by breaking of the H-bonding network. Effects of polar, aprotic solvent mixtures with water (Figure 4) show that the rate of hydrolytic deamination of 1-methylcytosine decreases with increasing cosolvent concentration, suggesting that at least two water molecules are necessary for the H-bonding network needed to form the tetrahedral intermediate. The enzyme-catalyzed reaction, on the other hand,

⁶ The equation $K_{tx} = k_{non}/(k_{cat}/K_m)$ assumes that k_{cat}/K_m provides a measure of the equilibrium constant for conversion of the free enzyme and substrate to the enzyme–substrate complex in the transition state for chemical transformation of the substrate. Transition state affinity is underestimated (K_{tx} is overestimated) if (A) k_{cat}/K_m is limited by diffusional encounter of the enzyme and substrate, (B) k_{cat} is limited by product release, as is often the case for dehydrogenases, or (C) there is a fundamental difference between the mechanisms of the uncatalyzed and enzymatic reactions (for a more detailed discussion, see ref 30).

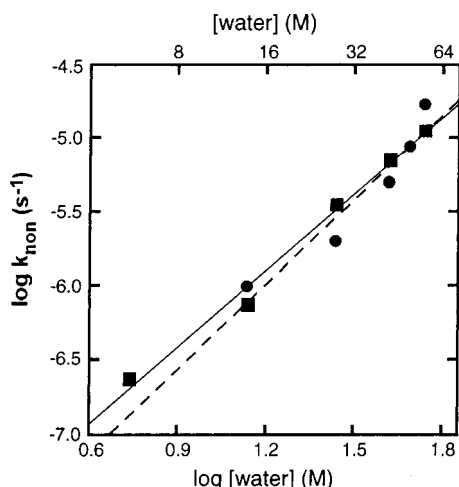


FIGURE 4: Effects of DMSO (●) and DMF (■) on the rate of spontaneous deamination of cytidine in neutral solution at 145 °C. The dotted and solid lines are based on linear regression analysis of the effects of DMF (slope = 1.7, $r = 0.99$) and DMSO (slope = 1.9, $r = 0.95$).

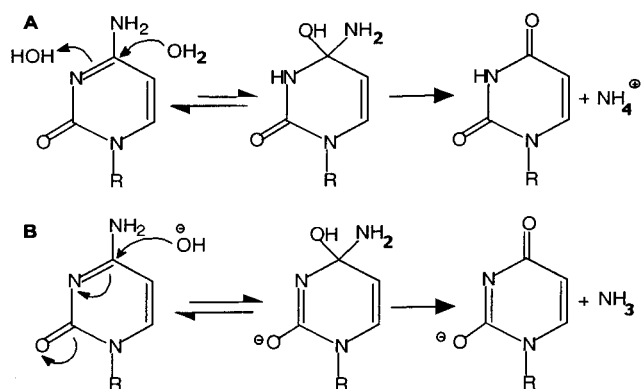


FIGURE 5: Differences in electron localization for spontaneous deaminations proceeding in (A) neutral and (B) alkaline solution.

already has a proton-transfer network in place that allows for efficient protonation and therefore reduces the commitment for C–N bond cleavage and shows a larger ¹⁵N kinetic isotope effect.

Because the mechanism of enzymatic cytidine deamination is proposed to involve Zn-coordinated hydroxide attack, the ¹⁵N isotope effect for the uncatalyzed reaction was remeasured at pH 12.5. Relative to the rate constant measured at pH 7.3 and 100 °C, the rate constant at pH 12.5 increased by a factor of 17 at this temperature, and the ¹⁵N isotope effect increased 1.7-fold, from 1.0021 to 1.0035. After hydroxide attack to form the tetrahedral intermediate, electron density resides on the more electronegative oxygen on C-2, rather than on the N-3, which is unprotonated under these conditions (Figure 5). The back reaction, to remove the hydroxyl at C-4, occurs more easily under these alkaline conditions than in neutral solution, since proton transfers are not required for its elimination. These changes in electron localization cause the forward commitment to C–N bond cleavage to decrease, increasing the observed isotope effect (Figure 5).

For both the water and hydroxide reactions, the small ¹⁵N kinetic isotope effect observed rules out a concerted reaction

mechanism, since a concerted reaction would result in a large primary kinetic isotope effect. Therefore, both the uncatalyzed and the enzymatic reactions proceed by similar mechanisms involving a tetrahedral intermediate formed by the stepwise addition of OH and elimination of NH₃, although the commitment to C–N bond cleavage is greater for the uncatalyzed reaction.

ACKNOWLEDGMENT

We thank Dr. Steve Short for his help in purifying wild-type and mutant cytidine deaminases.

REFERENCES

1. Frick, L., MacNeela, J. P., and Wolfenden, R. (1987) *Bioorg. Chem.* 15, 100.
2. Wolfenden, R. V. (1969) *Nature* 223, 704.
3. Xiang, S., Short, S. A., Wolfenden, R., and Carter, C. W., Jr. (1996) *Biochemistry* 35, 1335.
4. Betts, L., Xiang, S., Short, S. A., Wolfenden, R., and Carter, C. W., Jr. (1994) *J. Mol. Biol.* 235, 635.
5. Xiang, S., Short, S. A., Wolfenden, R., and Carter, C. W., Jr. (1995) *Biochemistry* 34, 4516.
6. Xiang, S., Short, S. A., Wolfenden, R., and Carter, C. W., Jr. (1997) *Biochemistry* 36, 4768.
7. Smith, A. A., Carlow, D. C., Wolfenden, R., and Short, S. A. (1994) *Biochemistry* 33, 6468.
8. Carlow, D. C., Short, S. A., and Wolfenden, R. (1998) *Biochemistry* 37, 1199.
9. Carlow, D. C., Smith, A. A., Yang, C. C., Short, S. A., and Wolfenden, R. (1995) *Biochemistry* 34, 4220.
10. Snider, M. J., Gaunitz, S., Ridgway, C., Short, S. A. and Wolfenden, R. (2000) *Biochemistry* 39, 9746.
11. Snider, M. J., and Wolfenden, R. (2001) *Biochemistry* 40, 11364–11371.
12. Weiss, P. M., Cook, P. F., Hermes, J. D., and Cleland, W. W. (1987) *Biochemistry* 26, 7378.
13. Merkler, D. J., Kline, P. C., Weiss, P., and Schramm, V. L. (1993) *Biochemistry* 32, 12993.
14. Smith, A. A., Carlow, D. C., Wolfenden, R., and Short, S. A. (1994) *Biochemistry* 33, 6468.
15. Yang, C. C., Carlow, D. C., Wolfenden, R., and Short, A. A. (1992) *Biochemistry* 31, 4168.
16. Helfer, D. L., Hosmane, R. S., Leonard, N. J. (1981) *J. Org. Chem.* 46, 4803.
17. Northrop, D. B. (1977) in *Isotope Effects on Enzyme-Catalyzed Reactions* (Cleland, W. W., O'Leary, M. H., and Northrop, D. B., Eds.) pp 122–148, University Park Press, Baltimore, MD.
18. Cohn, W. E. (1949) *Science* 109, 377.
19. Rishavy, M. A., and Cleland, W. W. (2000) *Biochemistry* 39, 4569.
20. Hermes, J. D., Weiss, P. M., and Cleland, W. W. (1985) *Biochemistry* 24, 2959.
21. Rishavy, M. A., Cleland, W. W., and Lusty, C. J. (2000) *Biochemistry* 39, 7309.
22. Glasoe, P. K., Long, F. A., (1960) *J. Phys. Chem.* 64, 188.
23. Frick, L., Yang, C., Marquez, V. E., and Wolfenden R. (1989) *Biochemistry* 28, 9423.
24. Wolfenden, R. (1968) *Biochemistry* 207, 2409.
25. Cohen, R. M., and Wolfenden, R. (1971) *J. Biol. Chem.* 246, 7561.
26. Wilson, D. K., Rudolph, F. B., and Quioco, F. A. (1991) *Science* 252, 1278.
27. Jencks, W. P. (1975) *Adv. Enzymol. RAMB* 43, 296.
28. Hermes, J. D., Roeske, C. A., O'Leary, M. H., Morrison, J. F., and Cleland, W. W. (1982) *Biochemistry* 21, 5106.
29. Kline, P. C., Schramm, V. L. (1994) *J. Biol. Chem.* 269, 22385.
30. Wolfenden, R. (1972) *Acc. Chem. Res.* 5, 10.